File Cy.

BRL MR 2593

BRL

MEMORANDUM REPORT NO. 2593

THE SENSITIVITY OF DOUBLE BASE PROPELLANT BURNING RATE TO INITIAL TEMPERATURE

Richard C. Strittmater
Emma M. Wineholt
Hughes E. Holmes

February 1976

USA BALLISTIC RESEARCH LABORATORIES
ABERDEEN PROVING GROUND, MARYLAND

Destroy this report when it is no longer needed.
Do not return it to the originator.

Secondary distribution of this report by originating or sponsoring activity is prohibited.

Additional copies of this report may be obtained from the National Technical Information Service, U.S. Department of Commerce, Springfield, Virginia 22151.

The findings in this report are not to be construed as an official Department of the Army position, unless so designated by other authorized documents.

UNCLASSIFIED

SECURITY CLASSIFICATION OF THIS PAGE *(When Data Entered)*

REPORT DOCUMENTATION PAGE		READ INSTRUCTIONS BEFORE COMPLETING FORM
1. REPORT NUMBER BRL MEMORANDUM REPORT NO. 2593	2. GOVT ACCESSION NO.	3. RECIPIENT'S CATALOG NUMBER
4. TITLE *(and Subtitle)* The Sensitivity of Double Base Propellant Burning Rate to Initial Temperature		5. TYPE OF REPORT & PERIOD COVERED BRL Memorandum Report 6. PERFORMING ORG. REPORT NUMBER
7. AUTHOR*(s)* Richard C. Strittmater Emma M. Wincholt Hughes E. Holmes		8. CONTRACT OR GRANT NUMBER*(s)*
9. PERFORMING ORGANIZATION NAME AND ADDRESS USA Ballistic Research Laboratories Aberdeen Proving Ground, MD 21005		10. PROGRAM ELEMENT, PROJECT, TASK AREA & WORK UNIT NUMBERS 1T161102AH53-04
11. CONTROLLING OFFICE NAME AND ADDRESS US Army Materiel Development & Readiness Command 5001 Eisenhower Avenue Alexandria, VA 22333		12. REPORT DATE FEBRUARY 1976 13. NUMBER OF PAGES 34
14. MONITORING AGENCY NAME & ADDRESS*(if different from Controlling Office)*		15. SECURITY CLASS. *(of this report)* Unclassified 15a. DECLASSIFICATION/DOWNGRADING SCHEDULE
16. DISTRIBUTION STATEMENT *(of this Report)* Approved for public release; distribution unlimited.		
17. DISTRIBUTION STATEMENT *(of the abstract entered in Block 20, if different from Report)*		
18. SUPPLEMENTARY NOTES		
19. KEY WORDS *(Continue on reverse side if necessary and identify by block number)* Solid Propellant; Steady Burning; Temperature Coefficient; Temperature Profile Measurements; Thermocouples		

ssv/4589

20. ABSTRACT *(Continue on reverse side if necessary and identify by block number)*

The Parr-Crawford, overlapping zone, model of double base propellant combustion, has been programmed for the fizz burning process. Burning rate, surface temperature, and maximum fizz zone temperature are measured at nominal range conditions (1 atm, 293 K for a given propellant and used in the model to determine the pre-exponential factors in the two Arrhenius reaction rate equations. The values of these two factors are then held constant as initial temperature and pressure are varied. From these solutions, points on the curves of constant initial temperature (T_o)

DD FORM 1 JAN 73 1473 EDITION OF 1 NOV 65 IS OBSOLETE

UNCLASSIFIED

SECURITY CLASSIFICATION OF THIS PAGE *(When Data Entered)*

are plotted on a graph of the log burning rate (r) vs log pressure (P). From these graphs it can be observed from the slope and spacing of the lines whether a burning rate law of the form

$$r = C_o \exp(\sigma T_o) P^n$$

can be used to systematize the model solutions; i.e., if the lines are straight and the vertical distance between lines is proportional to the difference in initial temperature, then n and σ can be given constant values. In this equation, n is the burning rate exponent and is equal to the slope of the lines. If all the initial temperature dependence is concentrated in the exponential term, then σ can be defined as the initial temperature sensitivity of the burning rate. C_o then depends only on propellant composition.

Considering the pressure dependence of the burning rate, the solutions obtained for first and second order reactions in the fizz zone do fit this equation from 0.01 atmosphere to 100 atmospheres. The only parameter affecting the slope of the lines on the graphs of the logarithm of burning rate vs logarithm of pressure is the order of the reaction in the fizz zone. The value of the slope (n) is equal to one half of the order of reaction in the fizz zone. The dependence of σ on propellant parameters needs to be examined in more detail. All that can be said on the basis of the limited solutions obtained of the modified Parr-Crawford model is that the temperature coefficient varies inversely with the total reaction energy and varies directly with the gas phase activation energy. The dependence of σ on these parameters follows the equation given by R. L. Coates* from laminar flame theory, within a few percent, in the range compared.

The burning rate, surface temperature and maximum fizz zone temperature are measured in a combustion chamber that has been constructed to optimize photography of the burning surface and the adjustment of initial temperature of the propellant sample over a wide range. The chamber is constructed to provide inert atmospheres from 0.01 atmosphere to 10 atmospheres. Data is given for X-14, M2, M7, and M13 double-base propellants.

---

* *R. L. Coates, "An Analysis of a Simplified Laminar Flame Theory for Solid Propellant Combustion" COMBUSTION SCIENCE AND TECHNOLOGY (4) 1 (1971).*

TABLE OF CONTENTS

LIST OF ILLUSTRATIONS

LIST OF ILLUSTRATIONS

I. INTRODUCTION

Much can be learned about the sensitivity of propellant burning rate to ambient or initial temperature by relating the experimental work of the rocket engineer on initial temperature sensitivity to that of the interior ballistician. Figure 1 shows a series of pressure time curves for rocket motor firings. The initial temperature (T_o) and the burning area to throat ratio (K) are varied in these firings, while the equilibrium pressure (P) and burning rate (r) are measured.

For suitably small steps of initial temperature certain difference ratios can be formed while one or another parameter was held constant in these firings. For instance if the burning area to throat ratio (K) is held constant then

$$\left[\frac{\Delta \ln P}{\Delta T_o}\right]_K \quad \text{or} \quad \left[\frac{\Delta \ln r}{\Delta T_o}\right]_K$$

can be computed and in the limit of small ΔT_o these ratios are defined as π_K and π_r in the literature.

When the interior ballistic properties of gun propellants are determined, the closed, constant pressure bomb is used, and another family of curves is generated which appears in Figure 2.

This family of curves appears as straight lines on a log plot over limited pressure ranges and the familiar burning rate law, $r = bP^n$, can be used. In this equation r is the linear burning rate and P is the pressure. The slope of the lines in Figure 2 gives n.

Going one step further the level curves of Figure 2 suggest a burning rate law of the following form

$$r = C_o \exp(\sigma T_o) P^n$$

where T_o is the initial temperature and C_o and σ are constants that depend on propellant composition.

If all the burning rate sensitivity to initial temperature is assumed to be concentrated in the exponential then σ can be defined as the sensitivity of burning rate to initial temperature at constant pressure by the following expression

$$\sigma = \left[\frac{\partial(\ln r)}{\partial T_o}\right]_P .$$

The symbol σ is also referred to as the burning rate temperature coefficient. The temperature coefficient (σ) is related to the temperature sensitivities used by the rocket engineer by the following equation

$$\sigma = \pi_r - n\pi_K \quad .$$

In this work an attempt is made to relate the log burning rate vs log pressure curves obtained from solutions of the overlapping zone Parr-Crawford[1] model to the above burning rate law. It may then be possible to specify the important parameters controlling C_o and σ. In this report σ will always be given in percent change in burning rate per degree Kelvin.

II. THE MODEL

The Parr-Crawford model of double base propellant burning divides the steady combustion process into three zones called the foam, fizz and flame zones. At pressures below ten atmospheres in inert atmospheres, the flame does not develop and this steady burning state is called fizz burning. It is the fizz burning problem which is solved and discussed here.

In the original work of Parr and Crawford, they worked out some approximate solutions to their set of equations, and predicted a family of burning rate vs pressure curves similar to those obtained experimentally. These approximate solutions, at two different ambient propellant temperatures, along with the burning surface temperature vs pressure curve are given in Figure 3. It is interesting to note the large variation of surface temperature with pressure and the "low pressure hump" in the burning rate curves. Parr and Crawford suggested that the solving of the exact overlapping zone problem should be one of the first improvements undertaken on their approximate solution. To this end, the following equations for fizz burning have been programmed and solutions have been obtained.

The steady heat flow equation with source and convective terms can be written as:

$$\frac{d}{dy}\left(\lambda\frac{dT}{dy}\right) - M\frac{d}{dy}(CT) + MQ_a\frac{d\varepsilon_a}{dy} + MQ_b\frac{d\varepsilon_b}{dy} = 0 \qquad (1)$$

where $MQ_a\frac{d\varepsilon_a}{dy} + MQ_b\frac{d\varepsilon_b}{dy} = q$ (distributed reactive heat source).

---

[1] *R. G. Parr, and B. L. Crawford, Jr., "A Physical Theory of Burning of Double Base Rocket Propellants," Journal of Physics and Colloid Chemistry (54) 929 (1950).*

The zero order solid phase reaction can be written as:

$$M \frac{d\epsilon_a}{dy} = \beta_a \rho (1 - \epsilon_a) \exp(-A_a/T), \tag{2}$$

and the first order gas phase reaction can be written as:

$$M \frac{d\epsilon_b}{dy} = \beta_b (\epsilon_a - \epsilon_b) \rho_f \exp(-A_b/T) \tag{3}$$

where

$$\frac{1}{\rho_f} = \frac{1-\epsilon_a}{\rho} + \frac{(\epsilon_a - \epsilon_b)RT}{PW_a} + \frac{\epsilon_b RT}{PW_b}$$

and

T = Kelvin Temperature,

y = the space coordinate perpendicular to burning surface,

ϵ_a = fraction of the foam reaction completed,

ϵ_b = fraction of the fizz-flame reaction completed,

$\lambda = \lambda_s(1 - .833\ \epsilon_a)$ = thermal conductivity,

λ_s = thermal conductivity of the solid propellant,

M = mass burning rate (linear burning rate times density),

C = specific heat at constant pressure,

Q_a = overall heat of reaction in foam zone,

Q_b = overall heat of reaction in fizz-flame zone,

ρ = density of solid propellant,

β_a = frequency factor for foam reaction,

β_b = frequency factor for fizz flame reaction,

A_a = activation energy (foam reaction) divided by gas constant,

A_b = activation energy (fizz reaction) divided by gas constant,

R = universal gas constant,

P = pressure of reaction products,

ρ_f = the density of the mixture of solid and reaction products,

W_a = molecular weight of foam reaction products,

W_b = molecular weight of fizz flame reaction products.

Since M, Q_a and Q_b are constants the heat flow equation (1) can be integrated and the constant of integration evaluated by assuming the heat flux is zero when $\varepsilon_a = 0$ and $\varepsilon_b = 0$ at the ambient temperature ($T = T_o$) far from the burning surface. The division of one equation by another eliminates λ and puts the equations in the following form for programming and computer solution.

$$\frac{dU}{d\varepsilon_a} = \frac{F[U - \varepsilon_a - (Q_b/Q_a)\varepsilon_b]\exp(1/GU+H)}{(1 - .833\ \varepsilon_a)(1-\varepsilon_a)} \quad , \tag{4}$$

$$\frac{d\varepsilon_b}{d\varepsilon_a} = \frac{F}{J} \frac{(\varepsilon_a - \varepsilon_b)\exp[(-A_b/A_a-1)/GU+H]}{(1-\varepsilon_a)[1-\varepsilon_a + (\frac{\varepsilon_a+\varepsilon_b}{2})\ \frac{1}{K}(U + \frac{H}{G})]} \tag{5}$$

where ε_a is regarded as the independent variable up to $\varepsilon_a = .99999$ for the computation of U and ε_b, and

$$U \text{ (reduced temperature)} = \frac{C(T-T_o)}{Q_a} \quad ,$$

$$F = \frac{M^2C}{\lambda_s \beta_a \rho} \quad ,$$

$$G = \frac{Q_a}{CA_a} \quad ,$$

$$H = T_o/A_a,$$

$$J = \frac{M^2C}{\lambda_s \beta_b \rho} \quad ,$$

$$K = \frac{PW_bC}{\rho RQ_a} \quad ,$$

where it has been assumed that $W_a = 2_b$ in equation (5).

To get the computation started U is given the initial value of one half of one percent of the maximum value of U and the initial value of ε_a is approximately 10^{-14}. This starting assumption has been shown to have negligible effect on the solutions. At the point $\varepsilon_a = .99999$ in the temperature reaction profile the following equation, obtained by dividing the integrated form of equation (1) by equation (3), is used to compute the remainder of the temperature reaction profile with ε_b now the independent variable.

$$\frac{dU}{d\varepsilon_b} = \frac{J(U-\varepsilon_a - \frac{Q_b}{Q_a}\varepsilon_b)[1-\varepsilon_a + \frac{(\varepsilon_a+\varepsilon_b)}{2}\frac{1}{K}(U+\frac{H}{G})]}{(1-.833\varepsilon_a)(\varepsilon_a-\varepsilon_b)\exp[(-A_b/A_a(GU+H)]} \qquad (6)$$

when ε_a is given its final value of 1 for this computation.

The values of U and ε_b obtained from equations (4) and (5) at ε_a=.99999 are used as initial values in equation (6) and U is computed as a function of ε_b out to ε_b=.999. The boundary condition at ε_b=.999 is obtained by specifying zero heat flux at the ε_b=.999 reaction fraction point. Under these conditions all the heat release within the boundaries neglecting the small starting flux goes into heating up the propellant and the final value of U = U_1 must be given by

$$0 = U_1 - 1 - \frac{Q_b}{Q_a}(.999). \qquad (7)$$

It must be admitted that the actual situation in the steady burning propellant must have some losses on the downstream side so that all the reaction energy does not heat the propellant, however, measured temperature profiles indicate that this assumption incurs small error. Then y can be computed through the region of $0<\varepsilon_a<.99999$ by numerically integrating equation (2) along with equations (4) and (5). Equation (2) is expressed in the following form for this computation

$$\frac{CM}{s}dy = \frac{F\exp(1/GU+H)\,d\varepsilon_a}{(1-\varepsilon_a)} \qquad (8)$$

The integration is carried out with respect to the expression on the right hand side so that all of the integrations will depend only on the dimensionless ratios given above. Then y is obtained by dividing the right side by the coefficient of dy.

Then to compute y from ε_a=.999 equation (3) is integrated along with equation (6). Equation (3) can be written in the following form to program and carry out this integration.

$$\frac{CM}{s}dy = \frac{J(\varepsilon_a+\varepsilon_b)(U+\frac{H}{G})\exp[A_b/A_a(GU+H)]}{2K(\varepsilon_a-\varepsilon_b)}d\varepsilon_b \; . \qquad (9)$$

It is important and interesting to note that the pressure (P) appears in just one parametric group (K) above, and (T_o) also appears in one group (H). These groups (K,H) can be given a series of values for a given value of the solid phase reaction energy parametric group (G), while adjusting the pre-exponential parameters (F and J) to match temperature conditions at the boundaries. A single steady burning experiment at standard range conditions (1 atmosphere, 293 K) is per-

formed to measure the boundary temperatures by viewing the burning surface with a high speed framing camera as the combustion zone burns past a very responsive thermocouple. The camera record is synchronized with the thermocouple output record. The emergence temperature (T_S) given by this experiment is assumed to be the fully reacted foam zone temperature of the model. The equation for U given at the fully reacted foam zone point gives

$$U_s = C(T_s - T_o)/Q_a \ .$$

Neglecting losses, the maximum value of U is given by

$$U_1 = C(T_1 - T_o)/Q_a .$$

This equation for U_1 can be substituted in the maximum temperature boundary condition given as equation 7 from which Q_b can be evaluated.

It is assumed here that β_a and β_b are not a function of pressure or initial temperature and therefore that the values of F and J, determined in the one atmosphere experiment, remains constant as other points on the family of initial temperature curves on the burning rate vs pressure chart are obtained.

This approach requires only that we assume values for the two activation energies and the solid phase heat of reaction. From measurements and the literature we can determine the best values for the parameters assumed constant in the model which are C, λ_s, ρ, and W_b.

The specific heat of X-14 was measured from 0° to 70°C and is reported in BRL Memo Report No. 2227.[2] The specific heat increased from 1300 to 1450 joules/kg-K in this range. These values are within the range of the specific heats of the product gases of a similar type double base propellant described in the report of O. K. Rice and Robert Ginnell.[3] On the basis of these observations a value of 1400 joules/kg-K will be used as the average constant value of the specific heat in all states of the steady burning process. The other three constants describe a single state of the propellant and are not as difficult to justify since only the variation with temperature in the given state must be considered. The solid state density is taken as 1620 kg/M^3, W_b=23.4 and λ_s=.209 joules/sec M-K.

---

[2] *J. Richard Ward, "Determination of Specific Heat of X-14 Propellant by Differential Scanning Calorimetry", BRL Memo Report No. 2227, September 1972. AD# 906477L.*

[3] *O. K. Rice and Robert Ginnell, "The Theory of Burning of Double Base Rocket Powders", Journal of Physics and Colloid Chemistry, (54) 885 (1950).*

III. DISCUSSION

As the propellant parameters are varied to determine the effect on burning rate and temperature coefficient, curves of constant T_o are obtained. First Q_a was varied with no constraints. Figures 4, 5, and 6 show the marked effect of the solid phase heat of reaction on burning rate and temperature coefficient. The activation energies are 10,000 K for the solid phase and 40,000 K for the fizz zone. Figures 4, 5, and 6 show the level curves of T_o for solid phase heats of reaction of 60, 36 and 12 cal/gm.

As additional solutions are computed and graphs of level curves of T_o are plotted for selected values of Q_a and Q_b it becomes apparent that reducing Q_b has the same effect on burning rate and temperature coefficient as reducing Q_a. Another way of stating this is that the burning rate and temperature coefficient depend on the total energy (Q_a+Q_b) rather than on the way these heats are distributed in the solid and gas. This is illustrated in Figures 7, 8, and 9 in which the total energy is 408, 384, 360 cal/gm respectively. These energies are the same as in Figures 4, 5, and 6 respectively, however, the solid phase and gas phase heats of reaction are distributed differently. Compare Figures 4 and 7, and Figures 5 and 8 and Figures 6 and 9 and note the same total energy and the same burning rates and temperature coefficients.

In all of the results obtained no departure from the straight line relationship between ln r and ln P has been found in the fizz burning state of the modified Parr-Crawford model.

The dependence of σ on propellant parameters needs to be examined in more detail. All that can be said on the basis of the limited solutions obtained of the modified Parr-Crawford model is that the temperature coefficient (σ) varies inversely with the total reaction energy and varies directly with the gas phase activation energy (A_b). The dependence of σ on these parameters and n agrees well with the following equation,

$$\sigma = \left(1+n+\frac{A_b}{2T_1}\right)\frac{1}{T_1}$$ given by R. L. Coates,[4] where $T_1=T_o+Q/c$.

This equation for σ has been partially integrated to assist in obtaining the following equation,

$$r = 1.36 \times 10^{-4} P^n (T_o+Q/c)^{1+n} \exp[-A_b/2(T_o+Q/c)] \qquad (10)$$

where r is given in m/sec when Q is the total energy (Q_a+Q_b) expressed in MJ/kg and P in MN/m^2. The constant coefficient has been fitted to an X-14 burning rate measurement at standard conditions (1 atm. 293 K).

---

[4] *R. L. Coates, "An Analysis of a Simplified Laminar Flame Theory for Solid Propellant Combustion", COMBUSTION SCIENCE AND TECHNOLOGY (4) 1 (1971).*

The computed temperature profiles have the form shown in Figure 10. The profiles are shown for two values of the initial temperature and three values of pressure. The solid phase heat of reaction is 12 cal/gm and the fizz zone heat of the reaction is 348 cal/gm for all profiles.

A schematic diagram of the combustion chamber designed and constructed and now in use for measuring burning rates and temperature profiles is shown in Figure 11. The high speed motion picture camera shown in the diagram is used to detect the emergence of a very responsive foil thermocouple. The camera record is synchronized with the thermocouple record by a fiducial mark and 1000 hertz square waves recorded on the film and the tape record. The "emergence temperature" can then be obtained from the thermocouple record. A typical record obtained on X-14, double base propellant, with emergence time and temperature marked, is shown in Figure 12. This experiment was conducted in one atmosphere of argon at 295 K. The burning rate is .0015m/sec.

A few burning rate vs pressure data points that have been obtained, on X-14 propellant, have been superimposed on the graph of Parr-Crawford level curves of T_o which gave the best fit with the experimental points. This is shown in Figure 13. The experimental points have a slope of 0.6. If, in the Parr-Crawford model, the order of the fizz reaction is raised to second order, the slope of the log burning rate vs the log pressure curve is increased to one. It is, therefore, indicated that the modeling of a given pressure exponent (n) in the burning rate law is a matter of selecting the proper order of reaction in the fizz zone. Additional data on X-14, M2, M7, and M13 are plotted on Figures 14, 15, 16, and 17.

IV. CONCLUSIONS

The trends and relations exhibited by the Parr-Crawford model described in this report are summarized as follows:

1. Parr-Crawford fizz burning state can be described by this burning rate law:

$$r = 1.36 \times 10^{-4} P^n (T_o + Q/c)^{1+n} \exp[-A_b/2(T_o + Q/c)]$$

2. Pressure exponent (n) in burning rate law is obtained by dividing order of fizz reaction by two.

3. σ decreases with increasing reaction energy $(Q_a + Q_b)$.

4. σ increases with increasing fizz zone activation energy (A_b).

5. No "low pressure hump" observed in burning rate vs pressure curves as in Parr-Crawford approximate solutions.

6. Equation for σ, derived from simplified laminar flame theory, given above, by Coates correlates significant parameter effects determined in this study quite well (within a few percent).

There are two difficulties associated with looking for correlation between the relationships given by the model and the real world of propellant combustion. The first is that the model describes fizz burning and not the flame burning encountered at gun and rocket pressures where most of the closed bomb experimental work has been done. The second has to do with the fact that changes in propellant composition that change only one parameter at a time are very difficult to achieve in practice. When these facts are considered one can understand why we cannot just compare the heat of combustion, as a measure of Q_a+Q_b, in the model, and expect to see the same trends in burning rate and temperature coefficient in the JANNAF propellant manual as is predicted by the model described in this report. These considerations probably are the major factors in explaining the apparent discrepancy between the prediction of Parr-Crawford fizz burning theory and the fact that in double base propellants at rocket and gun pressures the temperature coefficient rises with increasing reaction energy.

REFERENCES

1. R. G. Parr and B. L Crawford, Jr., "A Physical Theory of Burning of Double Base Rocket Propellants," Journal of Physics and Colloid Chemistry (54) 929 (1950).

2. J. Richard Ward, "Determination of Specific Heat of X-14 Propellant by Differential Scanning Calorimetry", BRL Memo Report No. 2227, September 1972. AD# 906477L.

3. O. K. Rice and Robert Ginnell, "The Theory of Burning of Double Base Rocket Powders", Journal of Physics and Colloid Chemistry, (54) 885 (1950).

4. R. L. Coates, "An Analysis of a Simplified Laminar Flame Theory for Solid Propellant Combustion", COMBUSTION SCIENCE AND TECHNOLOGY (4) 1 (1971).

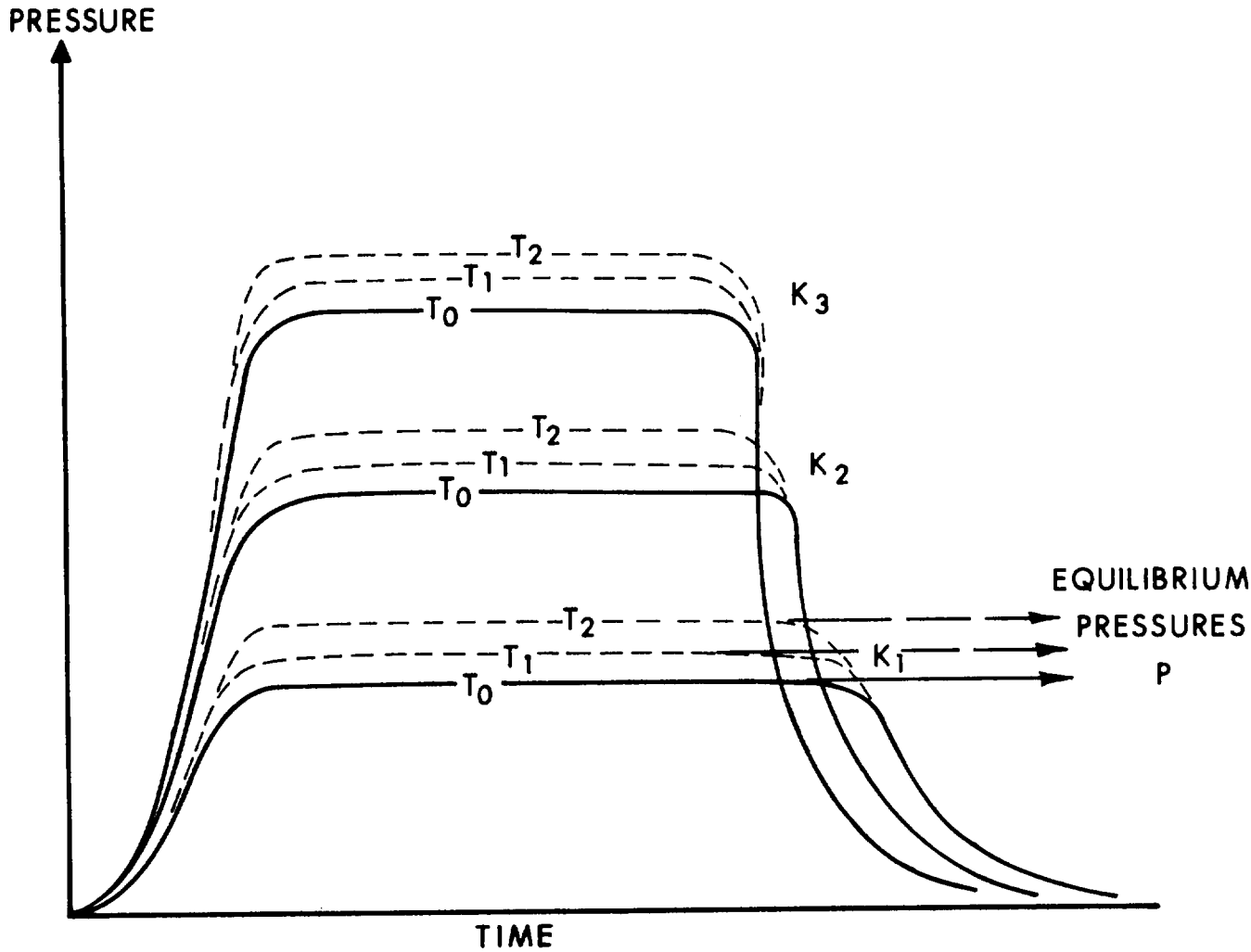

$$C_W = \frac{W}{PA_t}, \quad K = \frac{A_p}{A_t}$$

$$\left[\frac{\Delta \ell n P}{\Delta T}\right]_K \longrightarrow \pi_K$$

$$\left[\frac{\Delta \ell n r}{\Delta T}\right]_K \longrightarrow \pi_r$$

Figure 1. Pressure-time Curves from Rocket Motor Firings

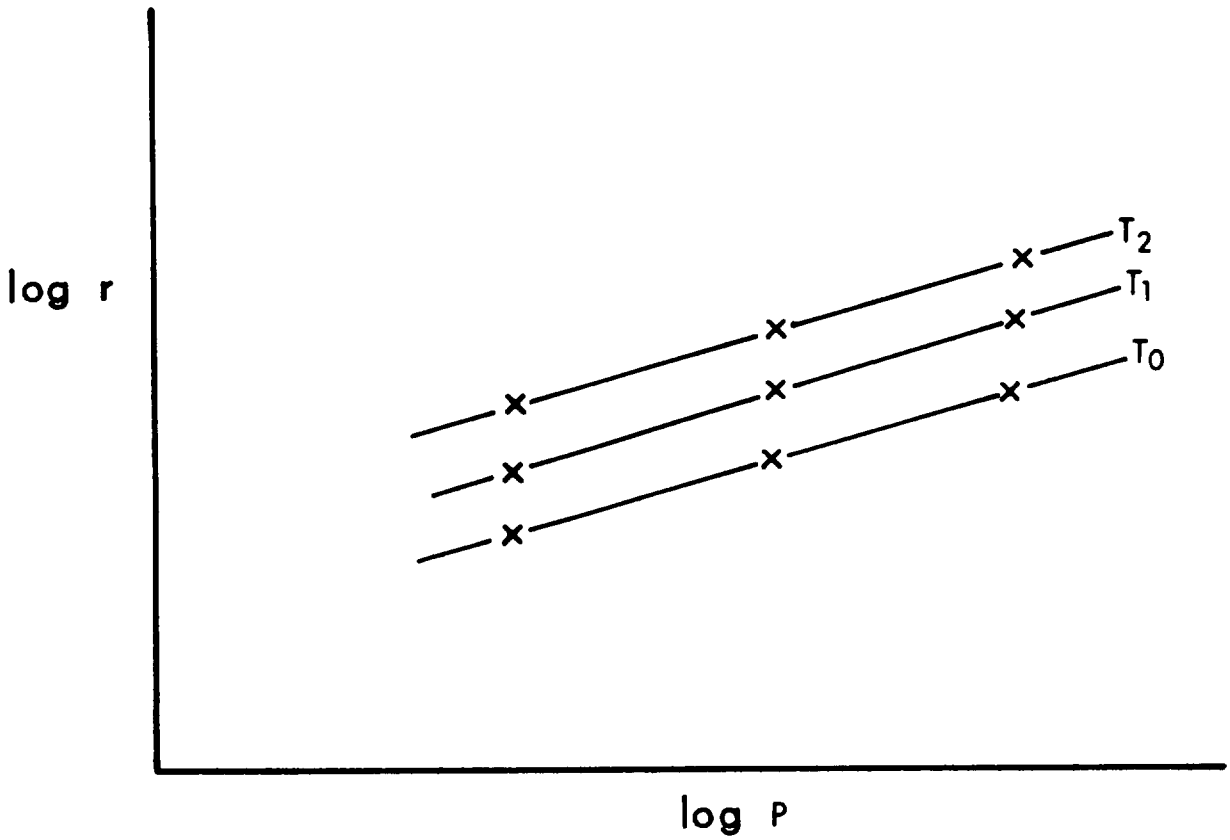

$$r = bP^n \qquad r = C_o e^{\sigma T_o} P^n$$

$$\left[\frac{\Delta \ell n r}{\Delta T}\right]_P \longrightarrow \sigma$$

$$\sigma = \pi_r - n\pi_K$$

Figure 2. Strand Burner Firing Curves used to Compute the Initial Temperature Sensitivity of Burning Rate

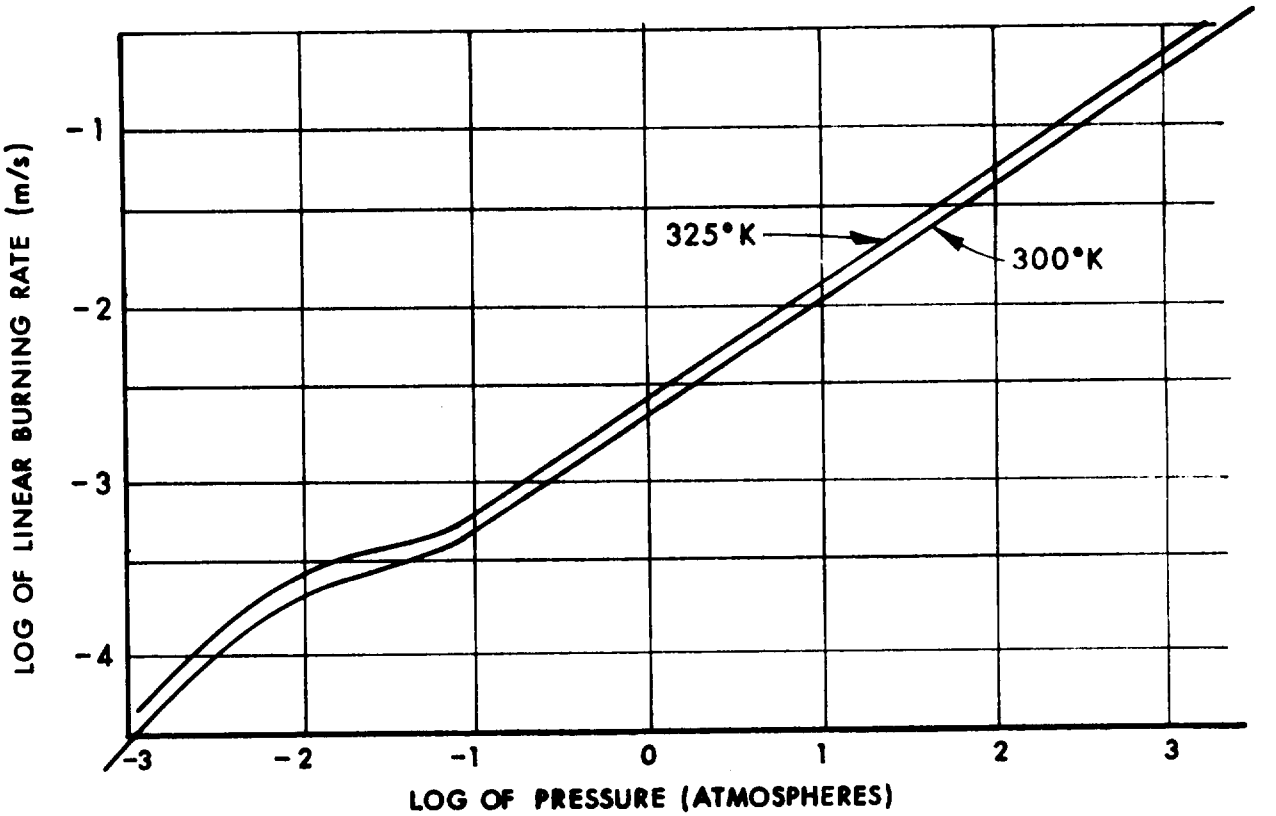

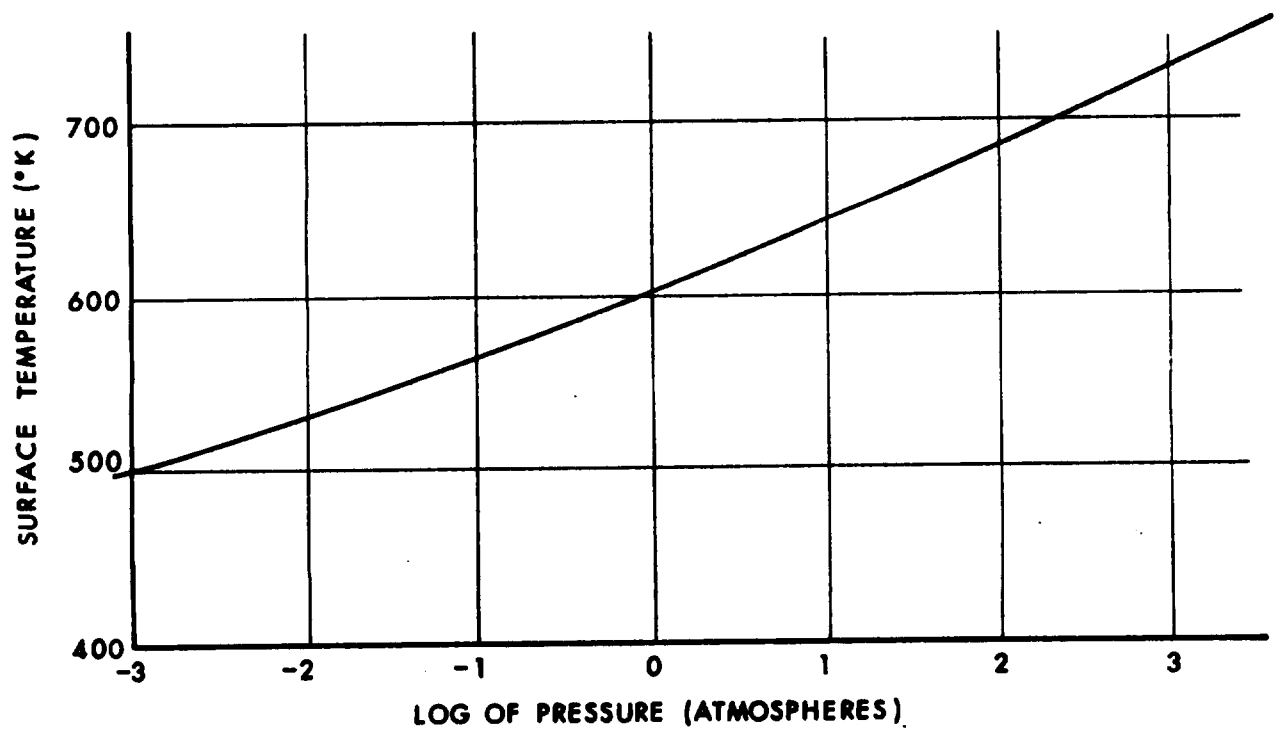

Figure 3. Computed Results of Approximate Solution of Parr-Crawford Theory for Fizz Burning

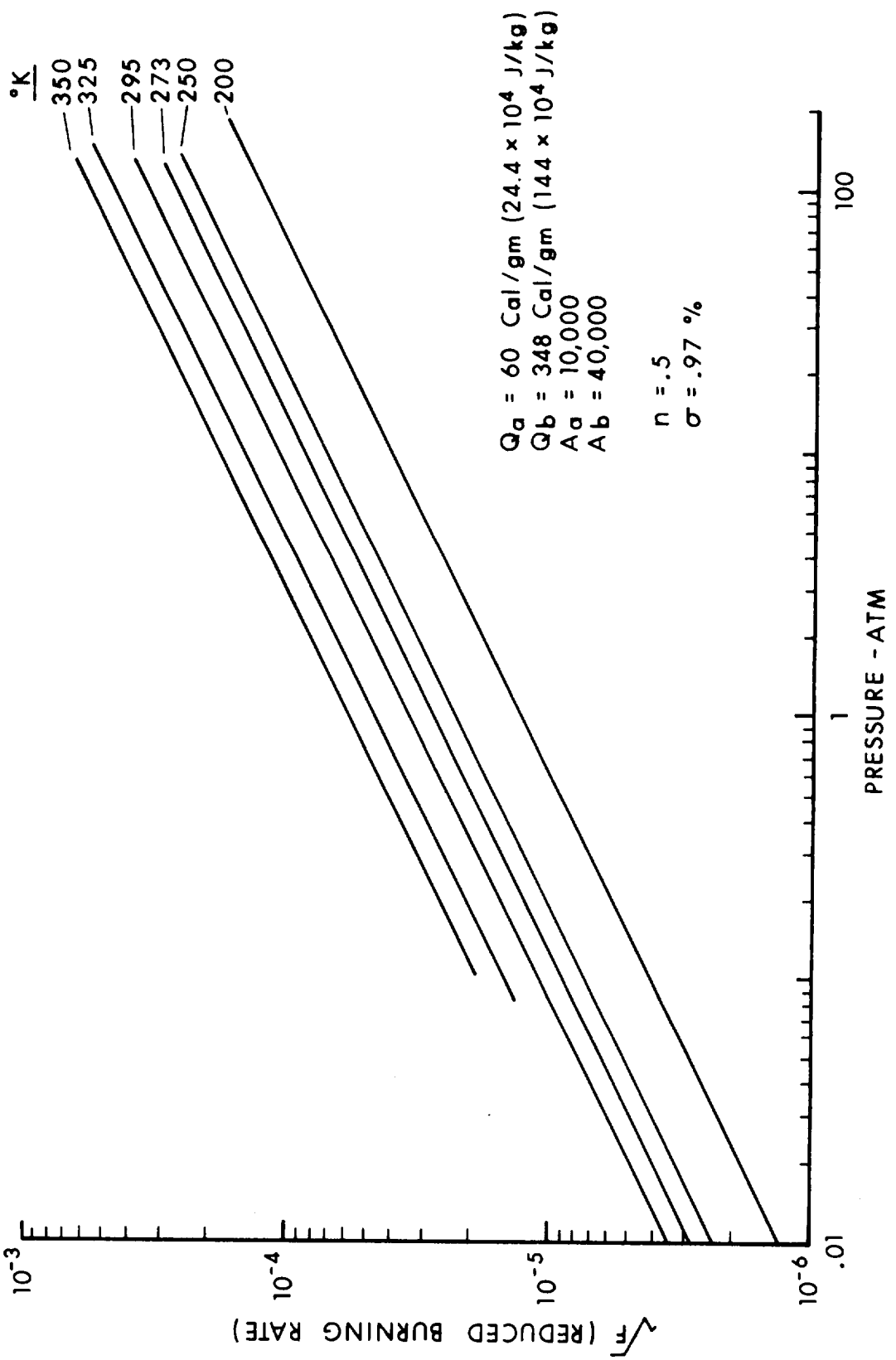

Figure 4. Computed Results of Overlapping Zone Parr-Crawford Theory for Fizz Burning with Parameters Noted

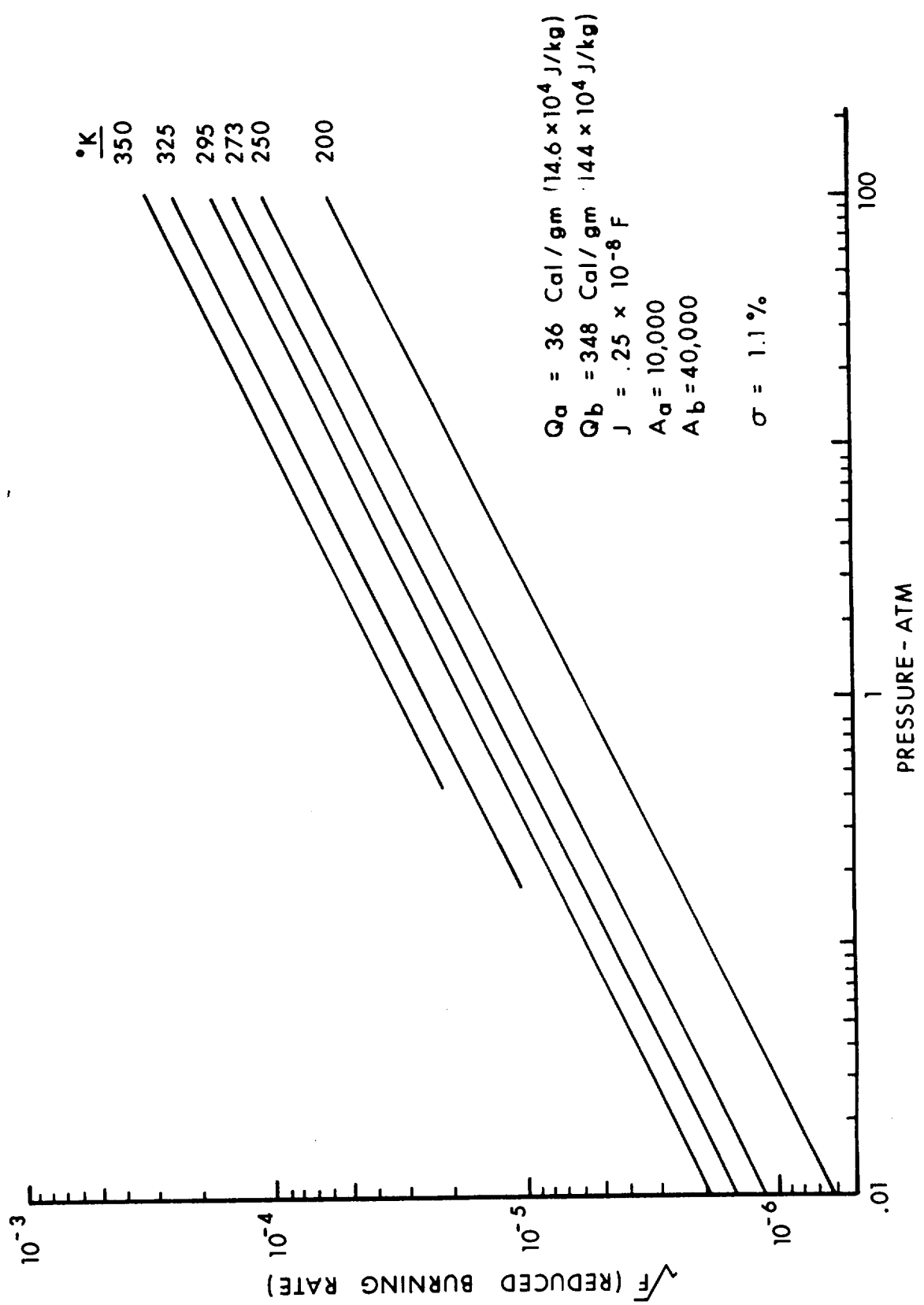

Figure 5. Computed Results of Overlapping Zone Parr-Crawford Theory for Fizz Burning with Parameters Noted

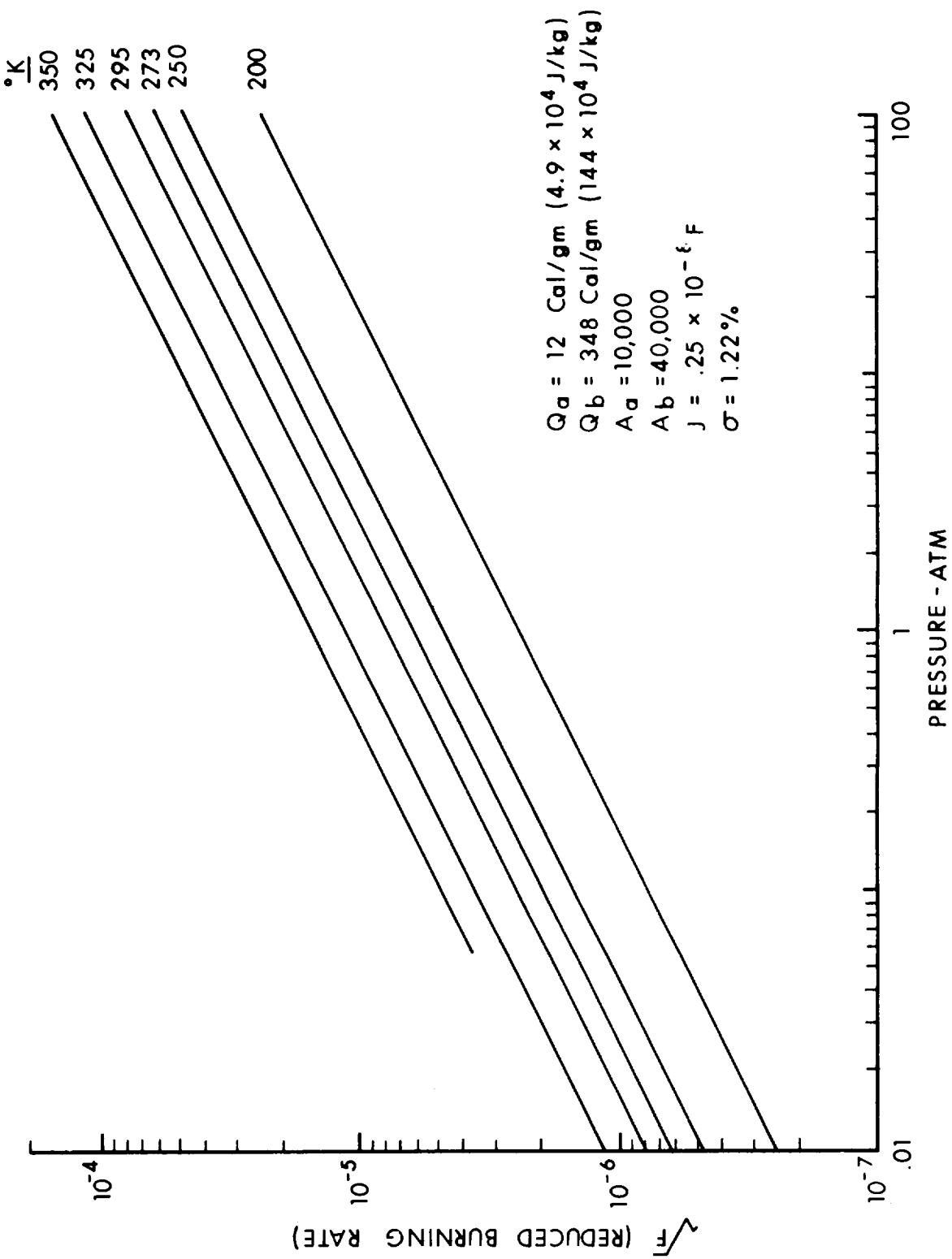

Figure 6. Computed Results of Overlapping Zone Parr-Crawford Theory for Fizz Burning with Parameters Noted

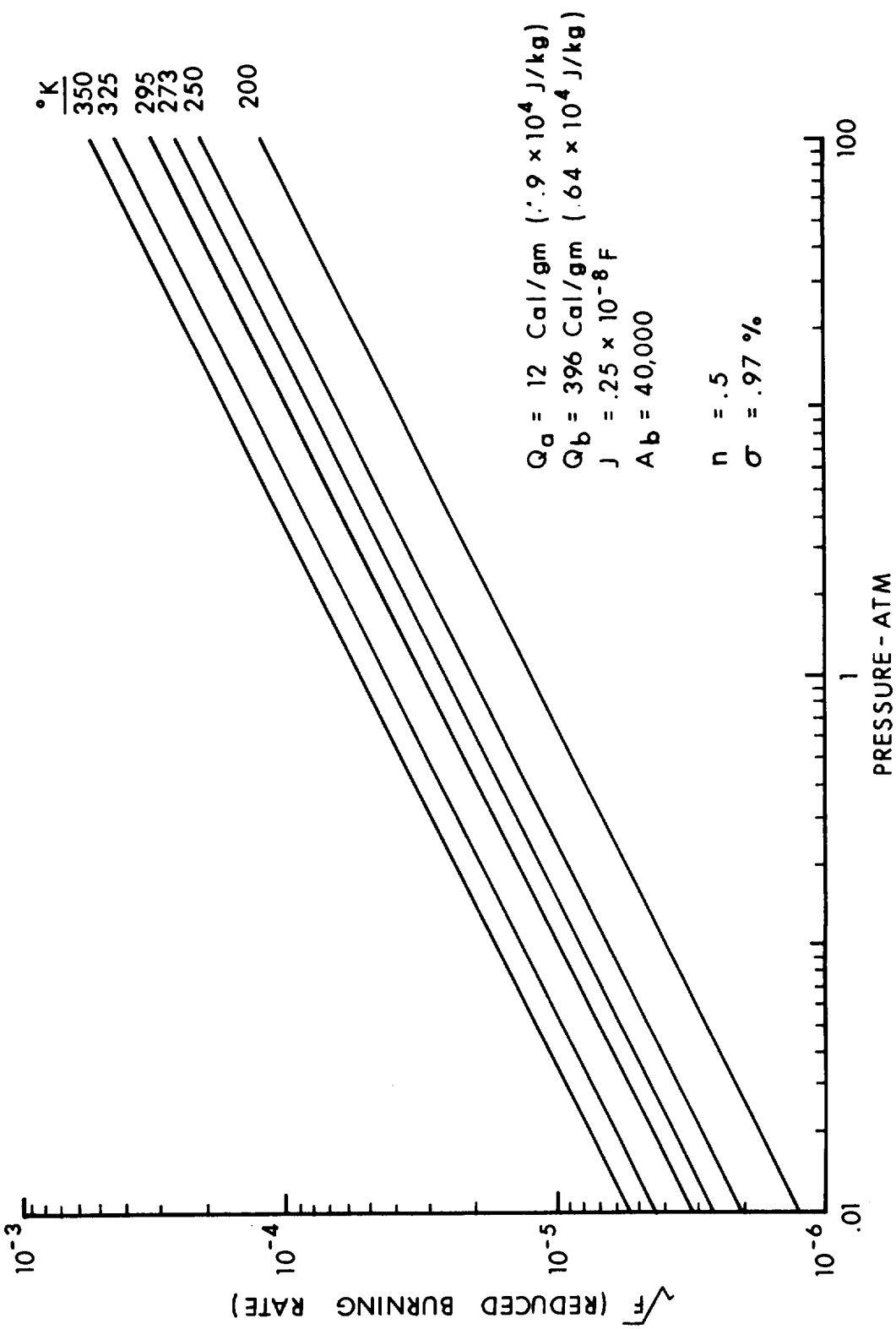

Figure 7. Computed Results of Overlapping Zone Parr-Crawford Theory for Fizz Burning with Parameters Noted

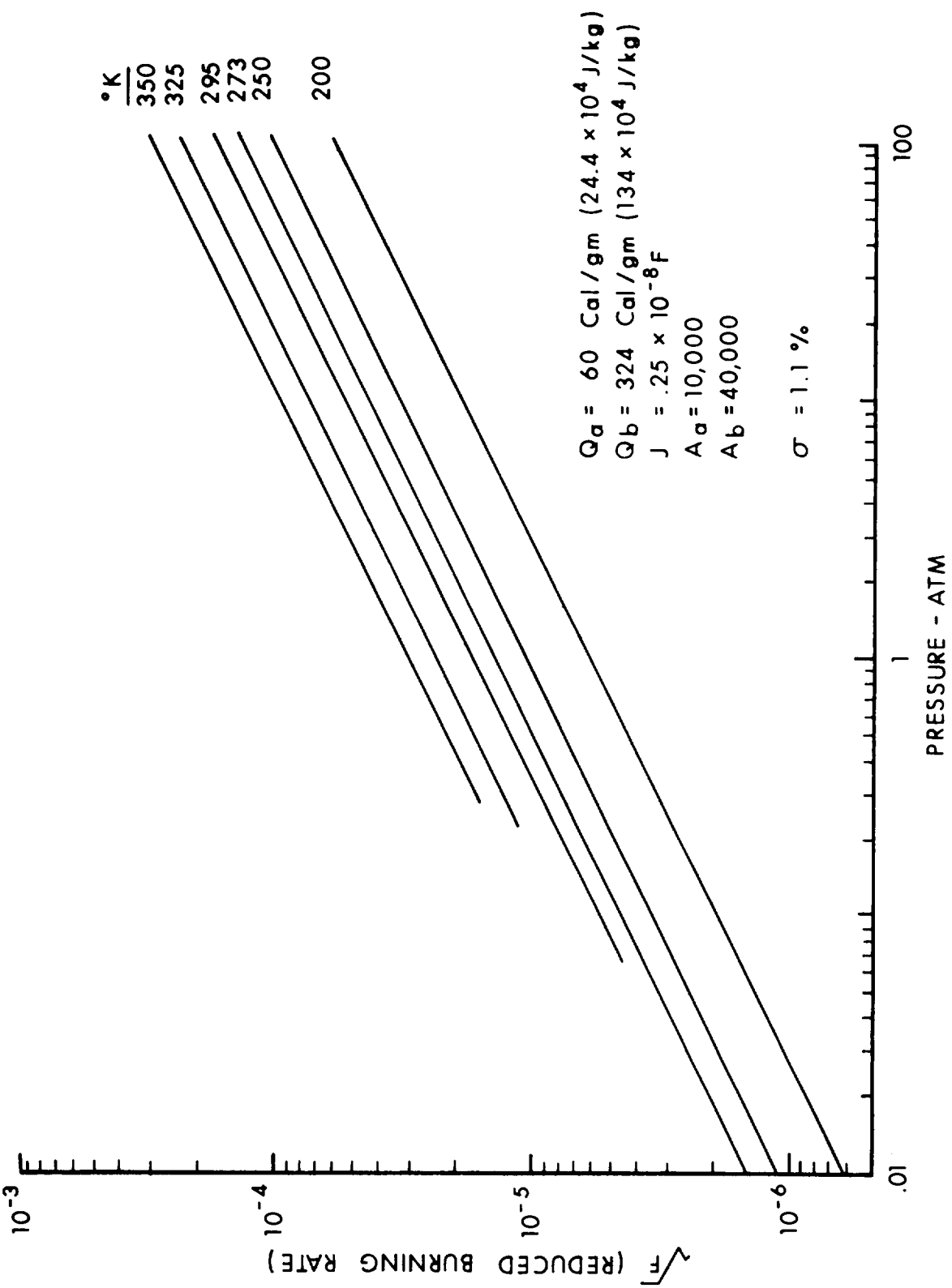

Figure 8. Computed Results of Overlapping Zone Parr-Crawford Theory for Fizz Burning with Parameters Noted

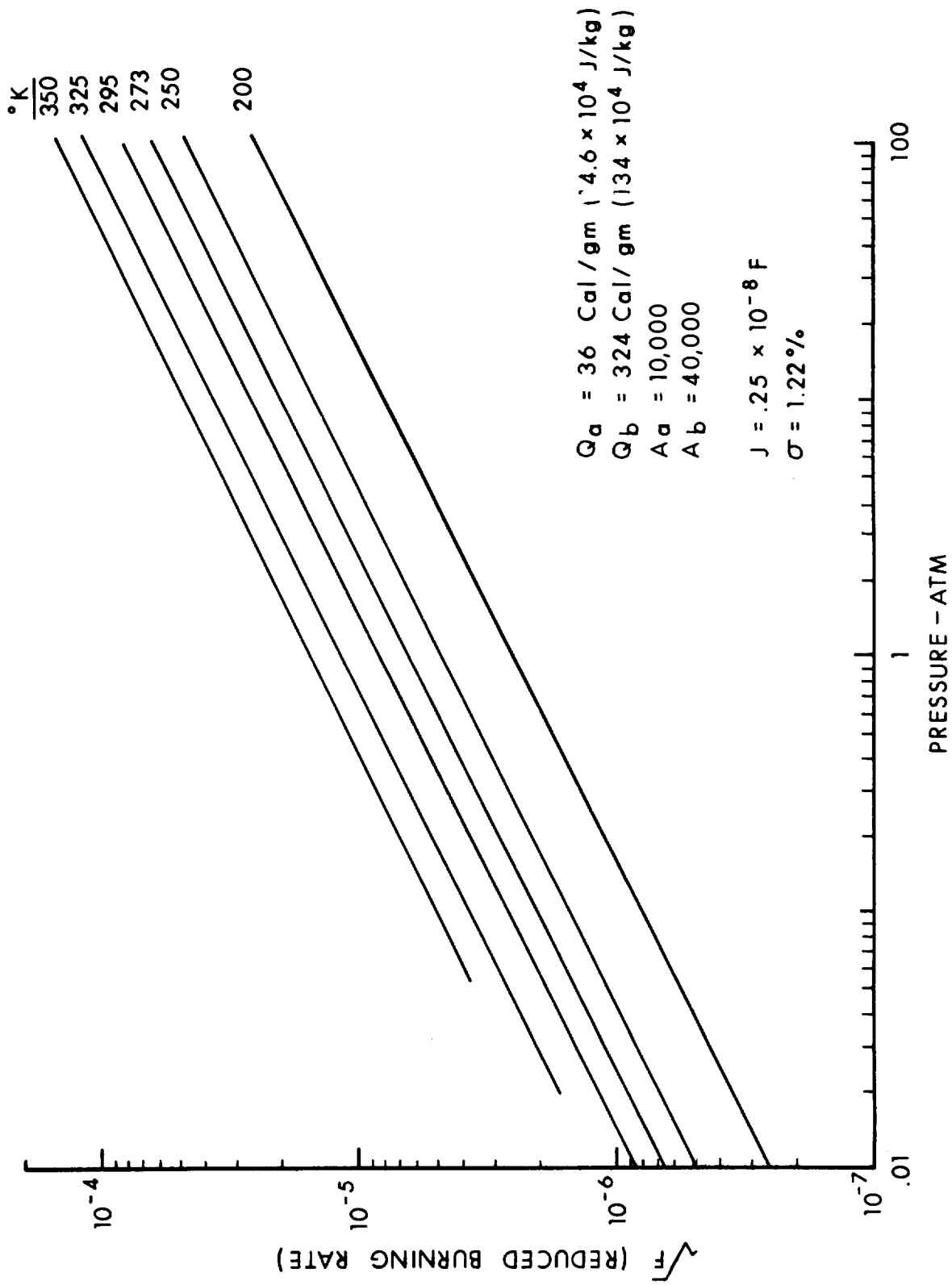

Figure 9. Computed Results of Overlapping Zone Parr-Crawford Theory for Fizz Burning with Parameters Noted

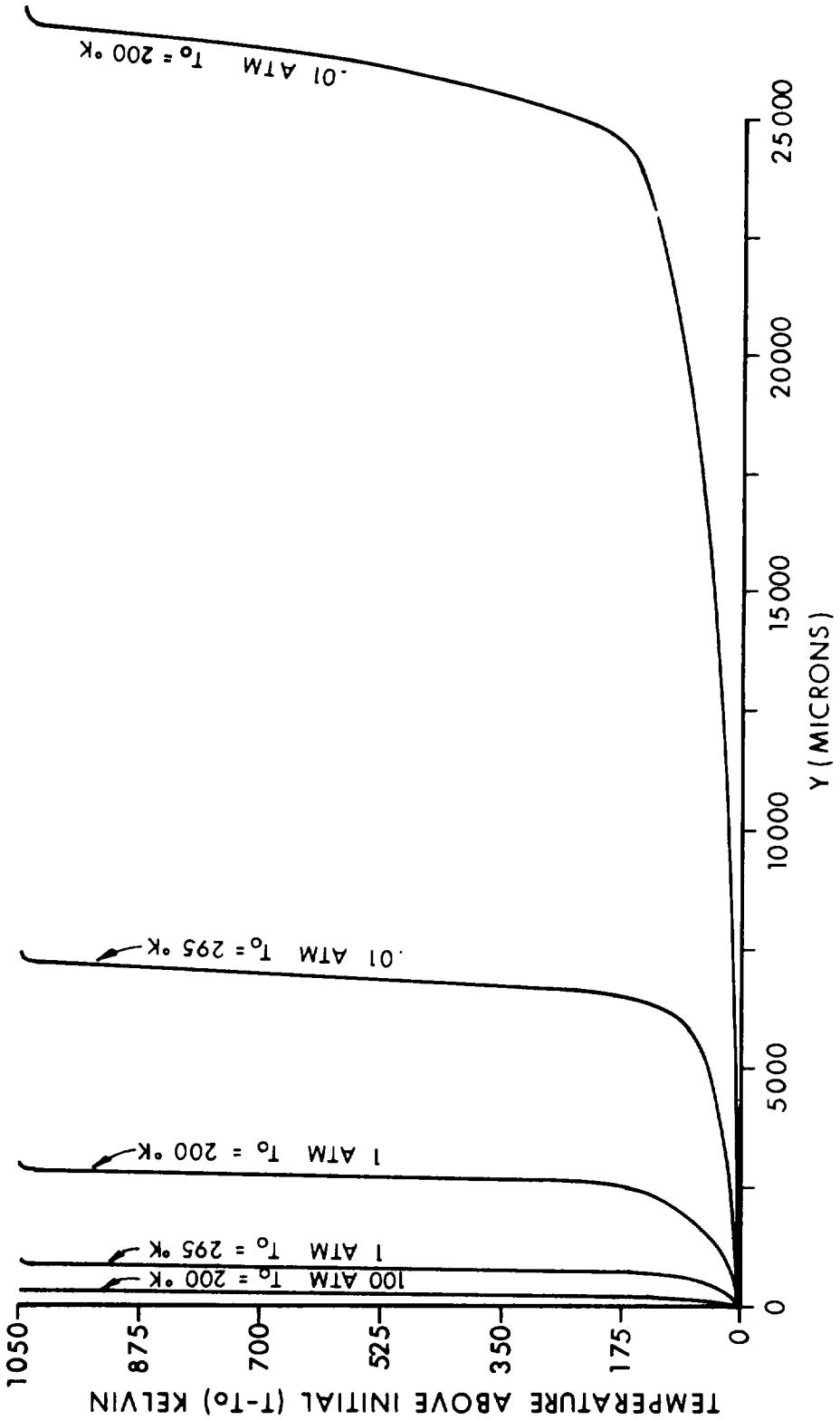

Figure 10. Temperature Profiles Obtained from Overlapping Zone Parr-Crawford Theory for Fizz Burning

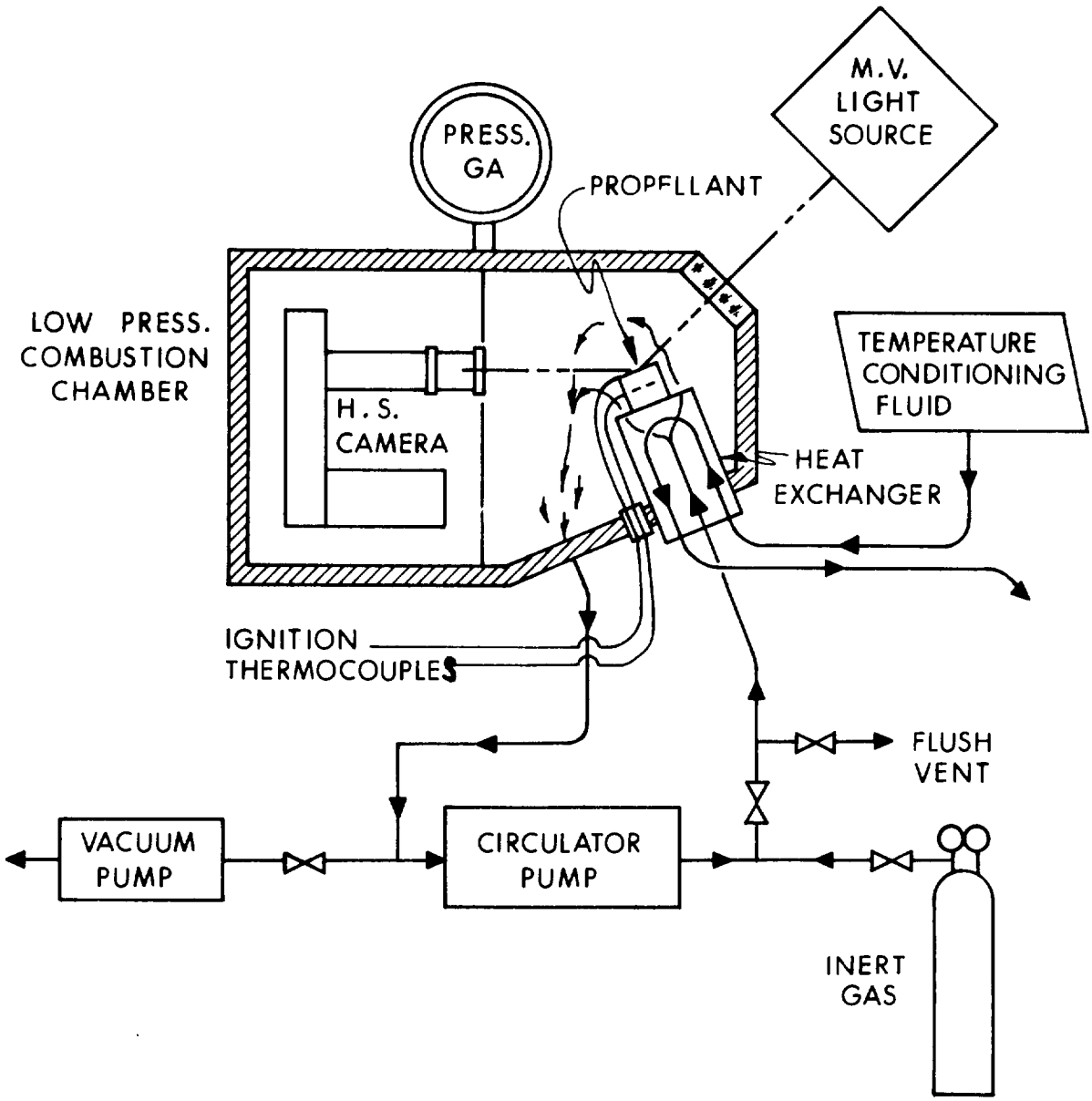

Figure 11. Block Diagram of Temperature Coefficient Experiment

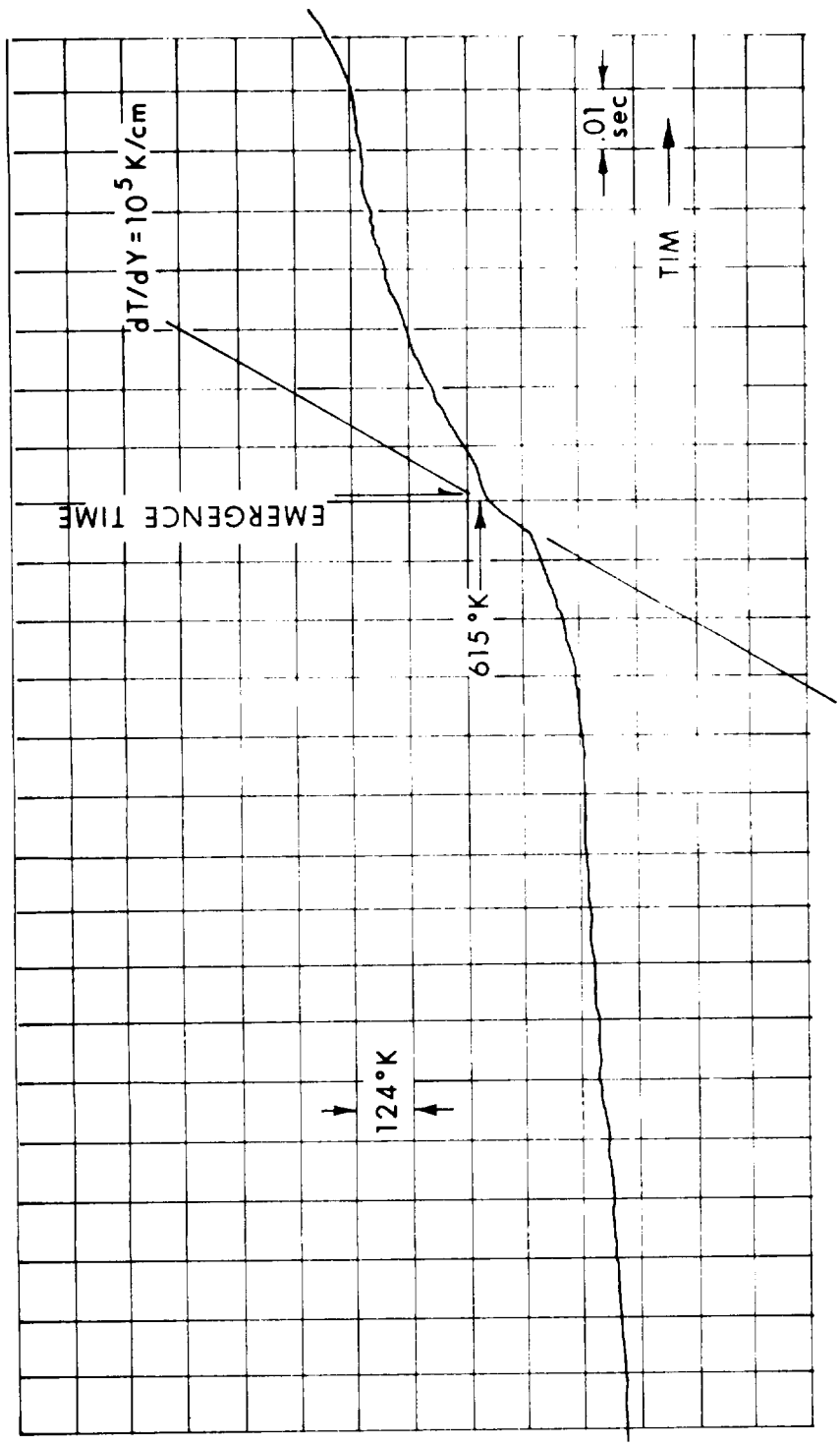

Figure 12. Temperature Profile Measured with Thermocouple in X-14 Double Base Propellant

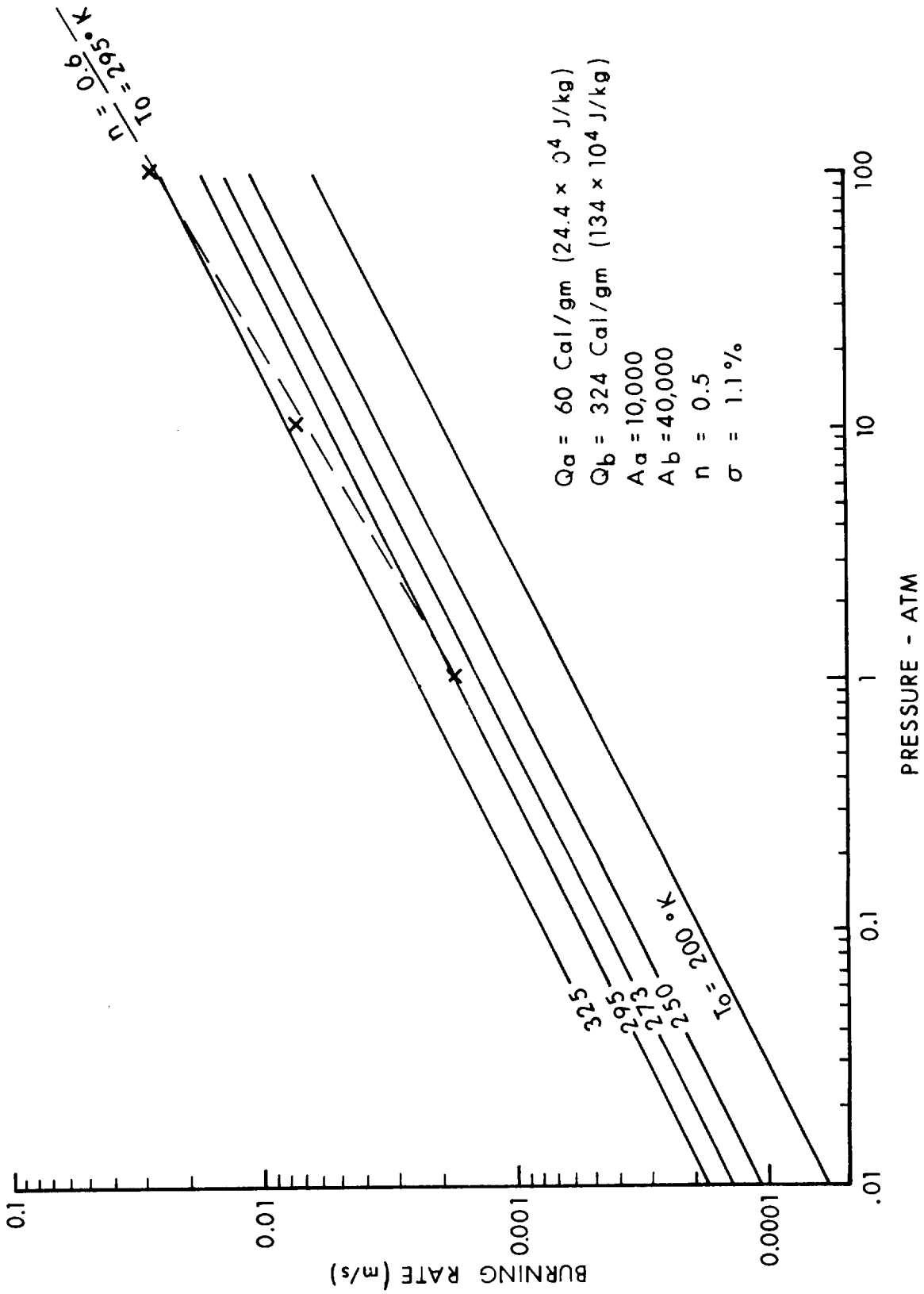

Figure 13. Overlapping Zone Parr-Crawford Theory Burning Rate Curves with Experimental Points on X-14 Double Base Propellant Superimposed

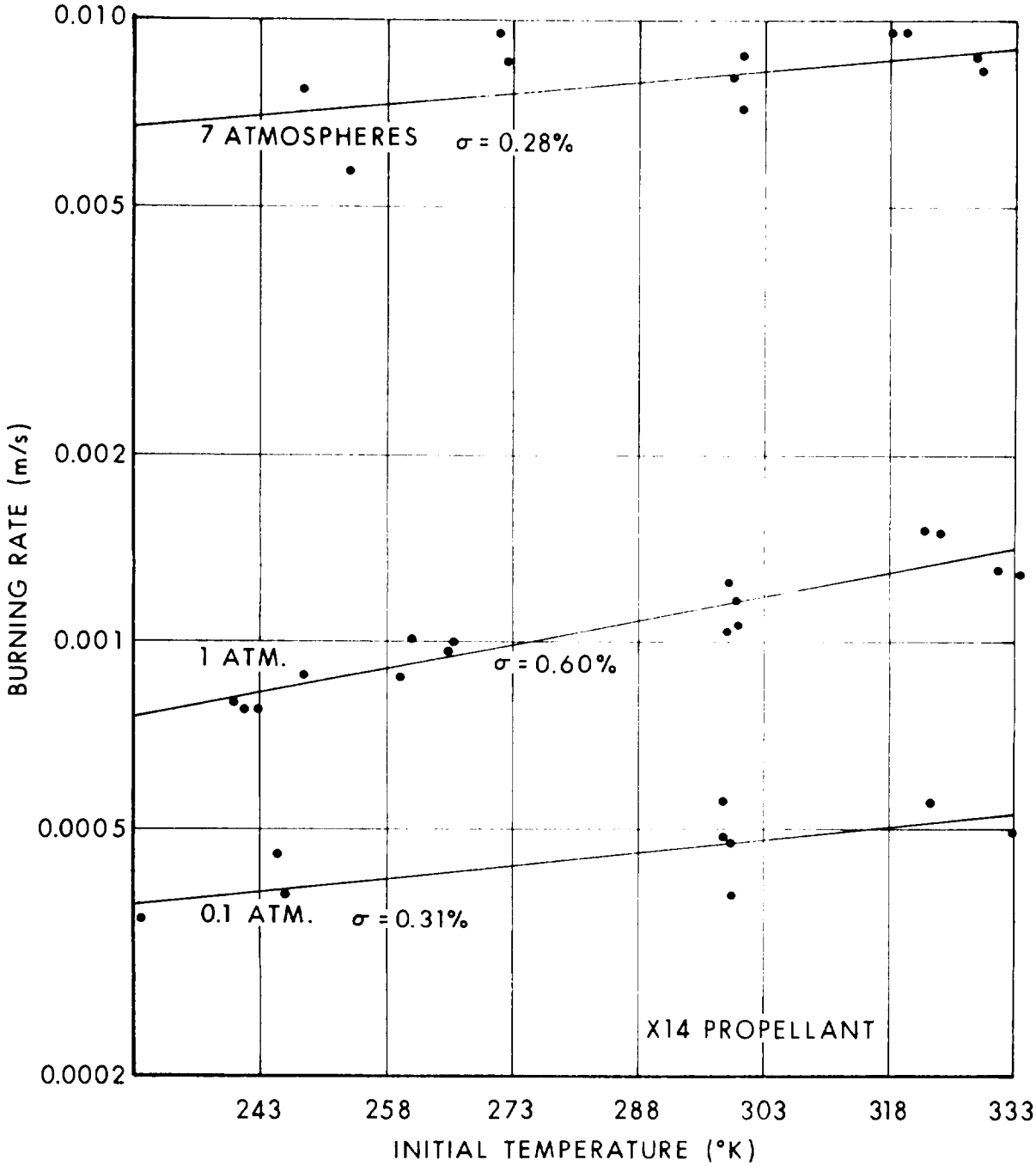

Figure 14. Burning Rate vs Initial Temperature for Various Pressures for X-14 Propellant

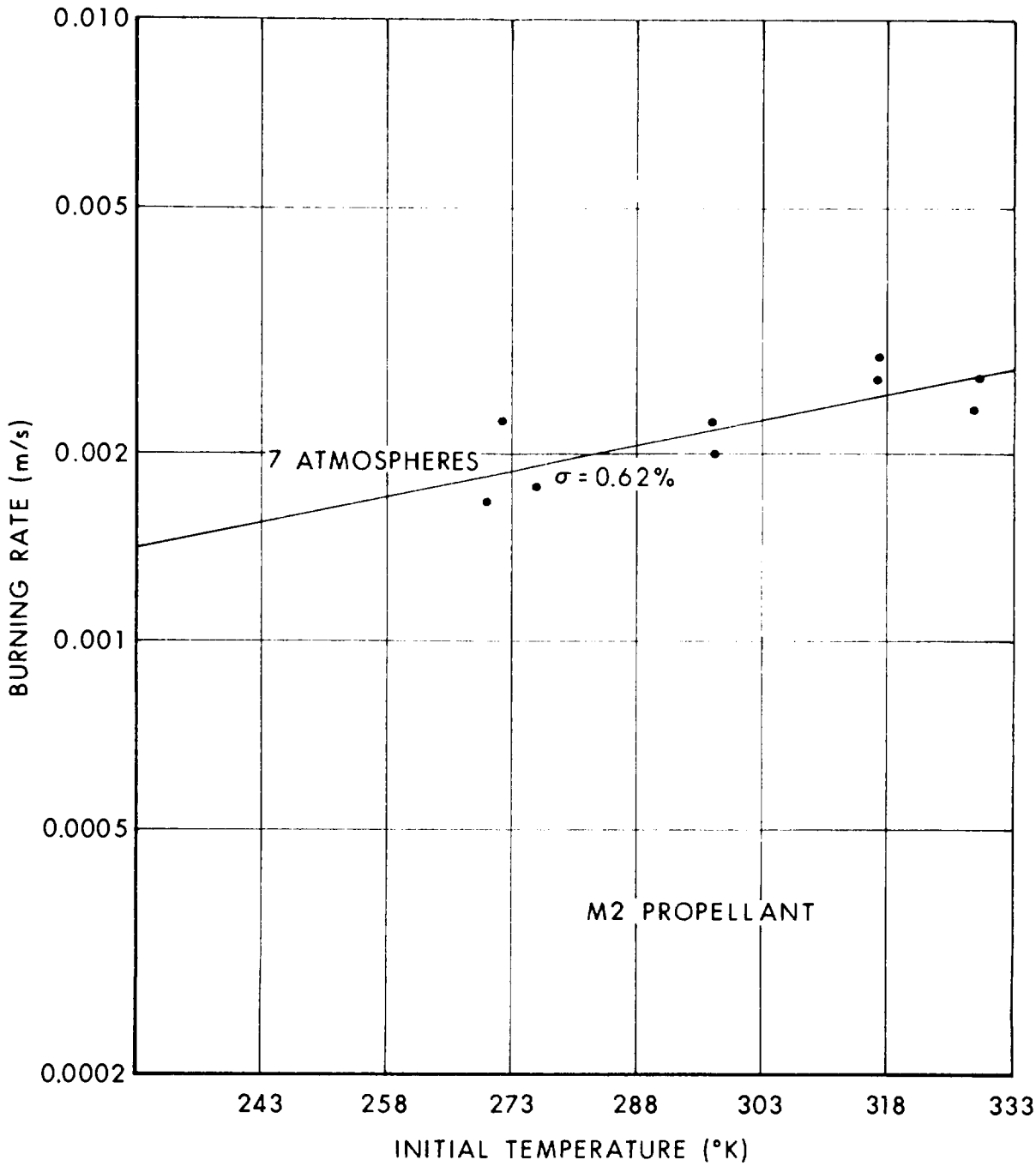

Figure 15. Burning Rate vs Initial Temperature at Seven Atmospheres for M2 Propellant

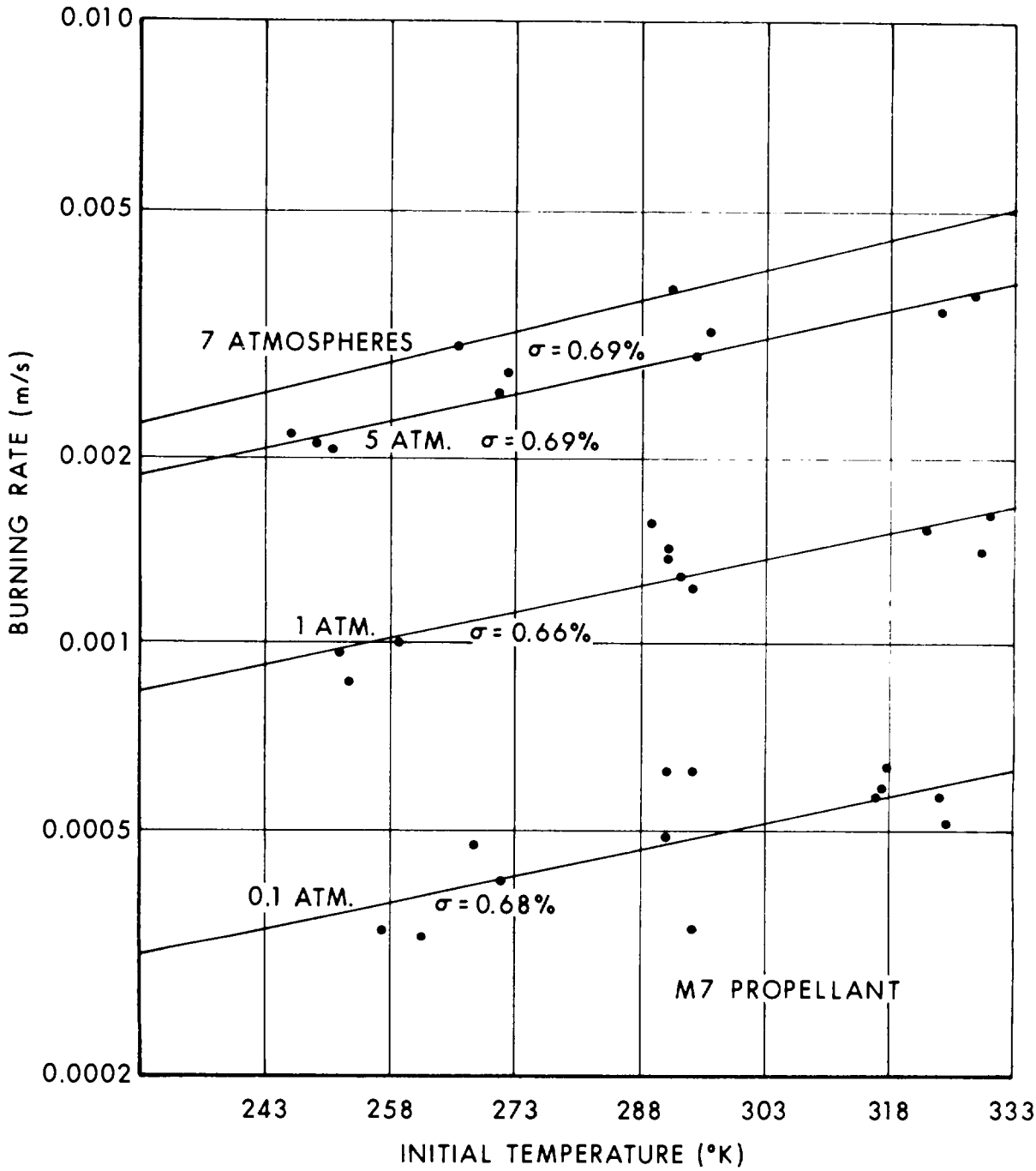

Figure 16. Burning Rate vs Initial Temperature at Various Pressures for M7 Propellant

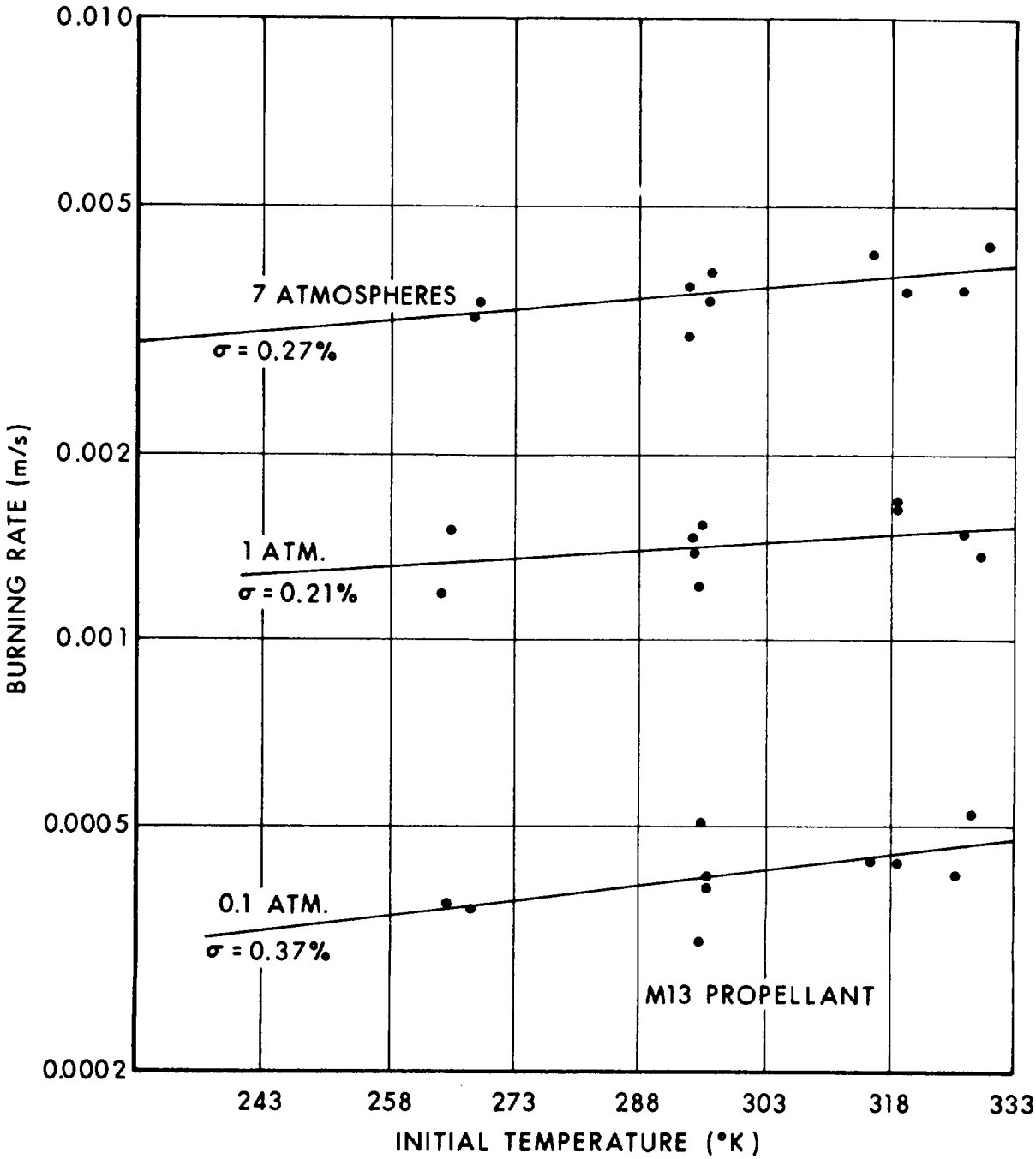

Figure 17. Burning Rate vs Initial Temperature at Various Pressures for M13 Propellant

DISTRIBUTION LIST

No. of Copies	Organization
12	Commander Defense Documentation Center ATTN: DDC-TCA Cameron Station Alexandria, VA 22314
1	Director Institute for Defense Analysis ATTN: Dr. H. Wolfhard 400 Army-Navy Drive Arlington, VA 22202
1	Commander US Army Materiel Development and Readiness Command ATTN: DRCDMA-ST 5001 Eisenhower Avenue Alexandria, VA 22333
1	Commander US Army Aviation Systems Command ATTN: DRSAV-E 12th and Spruce Streets St. Louis, MO 63166
1	Director US Army Air Mobility Research and Development Laboratory Ames Research Center Moffett Field, CA 94035
1	Commander US Army Electronics Command ATTN: DRSEL-RD Fort Monmouth, NJ 07703
1	Commander US Army Missile Command ATTN: DRSMI-R Redstone Arsenal, AL 35809
1	Commander US Army Tank Automotive Logistics Command ATTN: DRSTA-RHFL Warren, MI 48090
2	Commander US Army Mobility Equipment Research & Development Command ATTN: Tech Docu Cen, Bldg 315 DRSME-RZT Fort Belvoir, VA 22060
1	Commander US Army Armament Command Rock Island, IL 61202
4	Commander US Army Frankford Arsenal ATTN: SARFA-PDC, Dr. Lannon SARFA-MDS, Mr. Dickey SARFA-MDS, Mr. Kucsan SARFA-MDP, Mr. Mitchel Philadelphia, PA 19137
2	Commander US Army Picatinny Arsenal ATTN: SARPA-VG, Dr. J. Picard SARPA-VG, Mr. Lenchitz Dover, NJ 07801
1	Commander US Army White Sands Missile Range ATTN: STEWS-VT White Sands, NM 88002
1	Commander US Army Harry Diamond Labs ATTN: DRXDO-TI 2800 Powder Mill Road Adelphi, MD 20783
1	Commander US Army Materials and Mechanics Research Center ATTN: DRXMR-ATL Watertown, MA 02172

DISTRIBUTION LIST

No. of Copies	Organization
1	Commander US Army Natick Research and Development Command ATTN: DRXRE, Dr. D. Sieling Natick, MA 01762
1	Commander US Army TRADOC Systems Analysis Activity ATTN: ATAA-SA White Sands Missile Range NM 88002
1	Commander US Army Research Office ATTN: Tech Lib P.O. Box 12211 Research Triangle Park, NC 27709
5	Commander US Naval Air Systems Command ATTN: AIR-5366 AIR-5367 AIR-604 (3 cys) Washington, DC 20360
3	Commander US Naval Ordnance Systems Command ATTN: ORD-0632 ORD-035 ORD-5524 Washington, DC 20360
1	Chief of Naval Research ATTN: ONR-429 Department of the Navy Washington, DC 20360
1	Commander US Naval Missile Center ATTN: Code 5632 Point Mugu, CA 93041
4	Commander US Naval Surface Weapons Center ATTN: Tech Lib Dahlgren, VA 22448
1	Commander US Naval Surface Weapons Center ATTN: Code 730 Silver Spring, MD 20910
4	Commander US Naval Weapons Center ATTN: Code 608 Mr. E. Price Dr. R. Derr Code 753, Tech Lib China Lake, CA 93555
1	Director US Naval Research Laboratory ATTN: Code 6180 Washington, DC 20390
1	Superintendent US Naval Postgraduate School ATTN: Tech Lib Monterey, CA 93940
2	Commander US Naval Ordnance Station ATTN: Dr. A. Roberts Tech Lib Indian Head, MD 20640
1	AFSC (DOL) Andrews AFB Washington, DC 20331
1	AFOSR (SREP) 1400 Wilson Boulevard Arlington, VA 22209
2	AFRPL (RPMCP) ATTN: Dr. R. Weiss Dr. R. Schoner Edwards AFB, CA 93523

DISTRIBUTION LIST

No. of Copies	Organization
1	Headquarters National Aeronautics and Space Administration ATTN: RPS RP Washington, DC 20546
1	Director NASA Scientific and Technical Information Facility ATTN: CRT P.O. Box 8757 Baltimore/Washington International Airport, MD 21240
1	Director National Aeronautics and Space Administration George C. Marshall Space Flight Center ATTN: Tech Lib Huntsville, AL 35812
1	Director Jet Propulsion Laboratory ATTN: Tech Lib 4800 Oak Grove Drive Pasadena, CA 91103
1	Director National Aeronautics and Space Administration John F. Kennedy Space Center ATTN: Tech Lib Kennedy Space Center FL 32899
1	Director National Aeronautics and Space Administration Langley Research Center ATTN: MS-185, Tech Lib Langley Station Hampton, VA 23365
1	Director National Aeronautics and Space Administration ATTN: MS-603, Tech Lib MS-86, Dr. L. Povinelli 21000 Brookpark Road Lewis Research Center Cleveland, OH 44135
1	Director National Aeronautics and Space Administration Manned Spacecraft Center ATTN: Tech Lib Houston, TX 77058
1	Aerojet Solid Propulsion Co. ATTN: Dr. P. Micheli Sacramento, CA 95813
1	ARO, Inc. ATTN: Mr. N. Dougherty Arnold AFS, TN 37389
1	Atlantic Research Corporation ATTN: Tech Lib Shirley Highway at Edsall Road Alexandria, VA 22314
1	Calspan Corporation P.O. Box 235 Buffalo, NY 14221
1	General Electric Company Flight Propulsion Division ATTN: Tech Lib Cincinnati, OH 45215
2	Hercules Inc. Allegany Ballistic Laboratories ATTN: Dr. R. Yount Tech Lib Cumberland, MD 21501

DISTRIBUTION LIST

No. of Copies	Organization
1	Hercules, Inc. Bacchus Division ATTN: Dr. M. Beckstead Magna, UT 84044
1	Lockheed Propulsion Company ATTN: Dr. N. Cohen P.O. Box 111 Redlands, CA 92373
1	McDonnell Douglas Corporation Missile and Space Systems Div ATTN: Tech Lib Santa Monica, CA 90406
1	The Martin-Marietta Corporation Denver Division ATTN: Res Lib P.O. Box 179 Denver, CO 80201
2	North American Rockwell Corp. Rocketdyne Division ATTN: Dr. C. Oberg Tech Lib 6633 Canoga Avenue Canoga Park, CA 91304
2	North American Rockwell Corp. Rocketdyne Division ATTN: Mr. W. Haymes Tech Lib McGregor, TX 76657
1	Thiokol Chemical Corporation Huntsville Division ATTN: Dr. D. Flanigan Tech Lib Huntsville, AL 35807
2	Thiokol Chemical Corporation Wasatch Division ATTN: Dr. John Peterson Tech Lib P.O. Box 524 Brigham City, UT 84302
1	TRW Systems Group ATTN: Mr. H. Korman One Space Park Redondo Beach, CA 90278
1	United Aircraft Corporation Pratt and Whitney Division ATTN: Tech Lib P.O. Box 2691 West Palm Beach, FL 33402
2	United Technology Center ATTN: Dr. R. Brown Tech Lib P.O. Box 358 Sunnyvale, CA 94088
1	Battelle Memorial Institute ATTN: Tech Lib 505 King Avenue Columbus, OH 43201
1	Brigham Young University Dept of Chemical Engineering ATTN: Prof. R. Coates Provo, UT 84601
2	California Institute of Technology ATTN: Prof. F. Culick Tech Lib 1201 East California Boulevard Pasadena, CA 91102
1	Case Western Reserve University Division of Aerospace Sciences ATTN: Prof. J. Tien Cleveland, OH 44135
2	Georgia Institute of Technology School of Aerospace Engineering ATTN: Prof. B. Zinn Prof. W. Strahle Atlanta, GA 30333

DISTRIBUTION LIST

No. of Copies	Organization
1	IIT Research Institute ATTN: Prof. T. Torda 10 West 35th Street Chicago, IL 60616
1	Director Applied Physics Laboratory The Johns Hopkins University Johns Hopkins Road Laurel, MD 20810
2	Director Chemical Propulsion Information Agency The Johns Hopkins University ATTN: Mr. T. Christian Tech Lib Johns Hopkins Road Laurel, MD 20810
1	Massachusetts Institute of Technology Dept of Mechanical Engineering ATTN: Prof. T. Toong Cambridge, MA 02139
1	Pennsylvania State University Dept of Mechanical Engineering ATTN: Prof. G. Faeth University Park, PA 16802
4	Princeton University Dept of Aerospace and Mechanical Sciences ATTN: Prof. M. Summerfield Prof. I. Glassman Dr. L. Cavney Tech Lib James Forrestal Campus Princeton, NJ 08540
2	Purdue University School of Mechanical Engineering ATTN: Prof. J. Osborn Prof. S. N. B. Murthy Lafayette, IN 47907
1	Rutgers-State University Dept of Mechanical and Aerospace Engineering ATTN: Prof. S. Temkin University Heights Campus New Brunswick, NJ 08903
1	Stanford Research Institute Propulsion Sciences Division ATTN: Tech Lib 333 Ravenswood Avenue Menlo Park, CA 94024
1	Stevens Institute of Technology Davidson Laboratory ATTN: Prof. R. McAlevy III Hoboken, NJ 07030
2	University of California Dept of Aerospace Engineering ATTN: Prof. S. Penner Prof. F. Williams La Jolla, CA 92037
1	University of Denver Denver Research Institute ATTN: Tech Lib P.O. Box 10127 Denver, CO 80210
2	University of Illinois Dept of Aeronautical Engineering ATTN: Prof. H. Krier Prof. R. Strehlow Urbana, IL 61803
1	University of Minnesota Dept of Mechanical Engineering ATTN: Prof. E. Fletcher Minneapolis, MN 55455
2	University of Utah Dept of Chemical Engineering ATTN: Prof. A. Baer Prof. G. Flandro Salt Lake City, UT 84112

DISTRIBUTION LIST

No. of Copies	Organization
	Aberdeen Proving Ground
	Marine Corps Ln Orc
	Dir, USAMSAA